NOAA Technical Memorandum NWS WR-138

A SIMPLE ANALYSIS/DIAGNOSIS SYSTEM FOR REAL TIME EVALUATION OF VERTICAL MOTION

Scott Heflick and James Fors
Scientific Services Division
Western Region Headquarters
Salt Lake City, Utah

February 1979

UNITED STATES DEPARTMENT OF COMMERCE
Juanita M. Kreps,
Secretary

NATIONAL OCEANIC AND ATMOSPHERIC ADMINISTRATION
Richard Frank,
Administrator

NATIONAL WEATHER SERVICE
Richard E. Hallgren,
Director

This Technical Memorandum has been reviewed and is approved for publication by Scientific Services Division, Western Region.

L. W. Snellman, Chief
Scientific Services Division
Western Region Headquarters
Salt Lake City, Utah

CONTENTS

FIGURES

EDITOR'S NOTE: This Technical Memorandum is the result of Mr. Fors noting a paper by Hoskins in the January 1978 RMS Quarterly Journal and recognizing its potential as an operationally useful technique for Western Region and other forecasters. He then engineered Hoskins' ideas and programmed the technique for operational use on our local AFOS computer.

Mr. Heflick, as a summer trainee assigned to Scientific Services Division from June-August 1978, carried out the operational testing of the Fors' program as part of his student-trainee responsibilities.

We, SSD, plan to compute daily the diagnostic vertical-motion charts discussed in this Technical Memorandum and make them available to Western Region forecasters through AFOS as soon as data transmissions on our AFOS system become reliable.

L. W. Snellman, Chief
Scientific Services Division

A SIMPLE ANALYSIS/DIAGNOSIS SYSTEM FOR REAL TIME EVALUATION OF VERTICAL MOTION

Scott Heflick and James Fors
Scientific Services Division, Western Region
Salt Lake City, Utah

ABSTRACT

A diagnostic vertical motion model using a simple, modified Cressman objective analysis technique and a new "one-level" version of the quasi-geostrophic omega equation is investigated. The program is designed to run on an AFOS-type minicomputer. The diagnosed vertical motion field is compared with satellite and precipitation data. The results are in good agreement with the observed data, except in data-poor areas and for weak, small-scale systems. Some applications of this technique to operational forecasting are discussed.

I. INTRODUCTION

Operational forecasters have realized for many years the importance of vertical motion in determining the birth and decay of weather systems. Qualitative or quasi-quantitative determination of vertical motion from synoptic reasoning is familiar to all operational forecasters [12], [3], [10]. Consideration of vorticity advection, temperature advection, divergence and convergence, differential heating, and orographic effects have long been used by the forecaster as aids in producing precipitation forecasts.

Several quantitative methods of determining vertical motion based on the equations of motion such as the kinematic method [9], adiabatic method [9] and vorticity method [3], have been used by the forecaster. These time-consuming methods are rarely used since the development of modern numerical weather prediction has made the use of such methods unnecessary. However, with the rapid growth in development of minicomputers in recent years and the installation of the AFOS system, the forecaster now has the means of rapidly producing locally generated

products such as vertical motion based on quantitative dynamical equations. The standard teaching and diagnostic vertical motion tool over the last few years has been the quasigeostrophic omega equation [5]. Its familiar results of associating vertical motion with differential vorticity advection and the Laplacian of temperature advection is the cornerstone of much of the synoptic reasoning used today. However, its quantitative value can be discerned only by the use of the computer since the contributions from temperature advection and vorticity advection tend to cancel each other [13]. Thus, determining the vertical motion by using only one term in the equation may not even yield the correct sign of the vertical motion.

Another problem with the omega equation is the fact that vertical derivatives are involved in diagnosing the vertical motion. Thus, multiple levels of data are required for its solution. Many synoptic case studies have been done using this equation [11], [8], and [1]. Krishnamurti [7] developed a very complete form of the omega equation which included effects due to moisture as well. However, all of these studies required detailed hand analyses of many fields at many levels and a lot of computer time. Thus, such a diagnostic technique has been of limited use to operational forecasters.

In a recent article by Hoskins, et al,[6], the omega equation was rederived to present it in a simpler form which could be interpreted synoptically on a constant pressure chart without making simplifying assumptions. Only heights and temperatures at one level are required to calculate w, thus simplifying the conventional two- (or more) layer vertical-motion models usually employed.

The purpose of this paper is threefold. First, to show that a simple vertical-motion model based on Hoskins' equation and a simple objective analysis technique can produce a reasonable vertical- motion field. Second, that utilization of this program on an AFOS-type minicomputer can provide the forecaster with useful, real-time diagnosed vertical motion in his forecast area. And finally, that the diagnosed w field gives more precise vertical motion estimates with better resolution than those currently produced by the prognostic LFM-II [2] model.

II. PROCEDURES

A. The w Equation

Hoskins [6] used a pressure-type vertical coordinate system defined by

$$Z = (R\Theta_0/gk)\left(1 - \left(\frac{p}{p_0}\right)^K\right). \qquad (1)$$

This vertial coordinate is the same as physical height in a dry adiabatic atmosphere. θ_o and P_o are standard values of potential temperature and pressure. R is the standard gas constant for dry air and K is a constant ($\sim 2/7$). One advantage of this system of coordinates is the simplifying of the thermal wind relationship which may be expressed as:

$$\frac{\partial u_g}{\partial z} = -\frac{g}{f\theta_o}\frac{\partial \theta}{\partial y} \tag{2a}$$

$$\frac{\partial v_g}{\partial z} = \frac{g}{f\theta_o}\frac{\partial \theta}{\partial x} \tag{2b}$$

where θ is the potential temperature and u_g and v_g are the components of the geostrophic wind.

In this system, the standard w-equation is written as

$$N^2\nabla_h^2 w + f^2\frac{\partial^2 w}{\partial z^2} = f\frac{\partial}{\partial z}\left(\vec{V}_g\cdot\nabla\zeta_g\right) - \frac{g}{\theta_o}\nabla_h^2\left(\vec{V}_g\cdot\nabla\theta\right). \tag{3}$$

N^2 is the so-called "Brunt-Vaisalla" frequency defined by

$$N^2 = \frac{g}{\theta_o}\frac{d\theta}{dz} \tag{4}$$

and ζ_g is the vertical component of the geostrophic vorticity. The first term on the r.h.s. of (3) is the differential vorticity advection and the second term is the laplacian of temperature advection.

The major difficulties in using this form of the w-equation were discussed earlier. However, (3) may be rewritten using the thermal wind relationship [6] as

$$N^2\nabla_h^2 w + f^2\frac{\partial^2 w}{\partial z^2} = 2\nabla\cdot\vec{Q} \tag{5}$$

where

$$\vec{Q} = (Q_1, Q_2) = \left(-\frac{g}{\theta_o}\left(\frac{\partial \vec{V}_g}{\partial x}\right)\cdot\nabla\theta, -\frac{g}{\theta_o}\left(\frac{\partial \vec{V}_g}{\partial y}\right)\cdot\nabla\theta\right). \tag{6}$$

Thus, on an f-plane in the quasi-geostrophic system, vertical velocity is forced only by the divergence of $\vec{Q}$.

For ease of understanding, let's establish an X-Y coordinate system at a given point on a 700-mb chart such that X is parallel to the temperature contours and Y points toward the cold air. Then, $(\partial\theta/\partial x)$ vanishes and (6) becomes

$$\vec{Q} = (Q_1, Q_2) = \left(-\frac{g}{\theta_o}\frac{\partial v_g}{\partial x}\frac{\partial \theta}{\partial y}, -\frac{g}{\theta_o}\frac{\partial v_g}{\partial y}\frac{\partial \theta}{\partial y}\right). \tag{7}$$

Therefore, Q_1 is related to the horizontal shear of the geostrophic wind and Q_2 is related to the confluence or diffluence of the flow. Thus,

$$\vec{Q} \propto \frac{1}{L} \nabla v_g \qquad (8)$$

where L is the separation of the temperature contours in this X-Y system.

The Q field can be estimated in this way on a synoptic, constant-pressure chart. For qualitative interpretation, a divergent Q-field implies sinking and a convergent Q-field implies rising motion.

An additional term is added to (5) if f is allowed to vary with latitude. Thus, on a β-plane

$$N^2 \nabla_h^2 w + f^2 \frac{\partial^2 w}{\partial z^2} = 2 \nabla \cdot \vec{Q} + \beta \frac{g}{\theta_0} \frac{\partial \theta}{\partial x} . \qquad (9)$$

This form of the w-equation is also useful in a quantitative sense. Since no vertical derivatives are involved on the r.h.s. of (9), only one atmospheric level is required. Thus, application of this equation to a minicomputer is quite straightforward.

B. The Vertical Motion Model

The diagnostic vertical motion model was based on equation (9). The program was written in Fortran IV language using standard, second order finite difference and relaxation techniques. The program was run on an Eclipse S-230, AFOS-type minicomputer. A rectangular grid covering the western United States and eastern Pacific from 100°W - 135°W and 30°N - 55°N with one-degree mesh size was used (see Figure 1). Seven-hundred millibar heights and temperatures at 38 radiosonde stations served as data input. The 700-mb level was chosen as it gives a good representation of the lower level vertical motion field. Also, the contribution from temperature advection is not masked by large thermal winds. Also, up to 12 bogus observations could be entered in at any location in order to supplement data-sparse areas or areas of significant synoptic interest. After all height and temperature data had been entered, values were interpolated to each grid point using a modified Cressman analysis.

In the standard Cressman analysis [4] a circle with a radius of length N originating at each grid point is established. Any observation point at a distance D_i from the grid point where $D_i \leq N$ is weighted and averaged with other observations in the circle. The data are interpolated to the grid point by

$$Z_p = \frac{\sum_i (w_i z_i)}{\sum_i w_i} \qquad (10a)$$

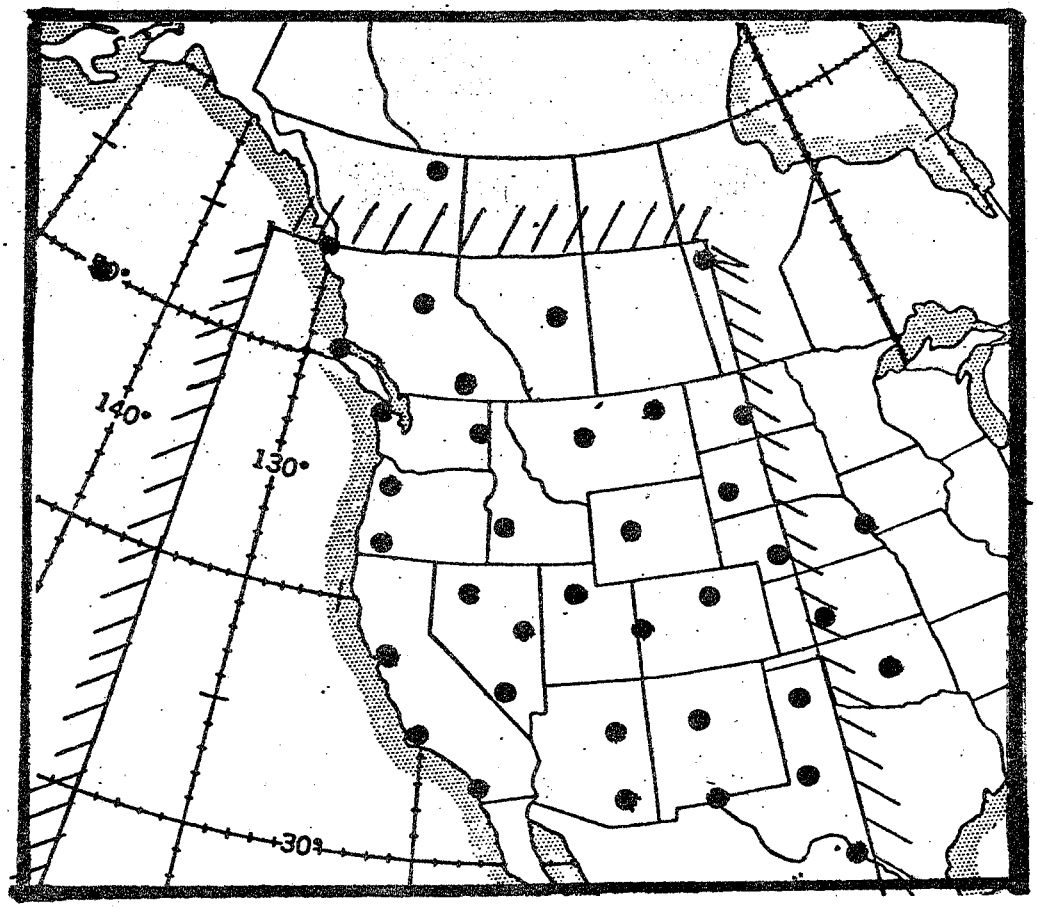

Figure 1. Upper-air stations used as input to analysis routine. The area of 1°x1° grid is also indicated.

$$W_i = \frac{N^2 - D_i^2}{N^2 + D_i^2} \qquad (10b)$$

where Z_i is any parameter at the ith observation point. Z_p is the value of the parameter at grid point P, and w_i is the weight of the observation Z_i. This interpolation method is repeated several times with decreasing values of N. The technique is usually used to modify a first-guess field.

The modified Cressman analysis [14] is based on the technique but differs in the following way. Rather than an arbitrary radius N being established, N is a variable and is defined as the distance between the grid point and one half the distance between the 7th and 8th closest observation point to the grid point. Also, only one sweep is made for interpolation of data rather than multiple scans as in the regular Cressman analysis and no first guess is used. This is repeated at each grid point until all grid points have been assigned specific values of the input parameters (height and temperature).

After the initial data were analyzed on the grid points, the r.h.s. of equation (9) was determined using finite difference approximations. If we approximate $(\partial^2 w/\partial z^2)$ on the l.h.s. of (9) using finite differences and assume that w=o at the surface and the tropopause, we may write (9) in the form

$$\nabla_h^2 W - CW = F. \qquad (11)$$

Here

$$F = \frac{1}{N^2}\left(2\nabla\cdot\vec{Q} + \beta\frac{g}{\theta_0}\frac{\partial\theta}{\partial x}\right) \qquad (12a)$$

and

$$C = \frac{2f^2}{N^2(\Delta z)^2} \qquad (12b)$$

where ΔZ was taken as 5000m. Equation (11) is readily solved using sequential relaxation. A residue tolerance of .01 cm/sec was used.

This model is a simple analysis-diagnostic system. Careful hand analysis of fields and the w-equation have been used successfully many times to diagnose vertical motion [1], [7], [11]. However, the usefulness of a simple objective analysis routine to initialize the model has not been investigated. The results of 4 case studies using this model are presented in the next section.

III. CASE STUDIES

a. July 20 - 21, 1978

On 00Z July 20, 1978, an upper-level short-wave trough was centered over northern Idaho. The trough moved progressively southeastward during the next 36 hours (see Figures 2a-d). By 12Z on the 21st the trough axis extended from the Colorado-Utah border to southeastern Arizona. Scattered, light precipitation occurred in Montana, Wyoming, southeastern Idaho, and Utah with maximum amounts in Montana and Wyoming where the upward vertical velocity (UVV) ahead of the trough was combined with orographic effects.

Figures 3a-d show the diagnosed vertical motion field (VMF) at 12-hour intervals for 00Z on the 20th, to 12Z on the 21st. Figure 3a shows a vertical motion maximum of greater than +2 cm s^{-1} ahead of the trough over central Idaho apparently due to PVA. UVV was indicated east of the trough throughout Idaho, Utah, Colorado, Arizona, New Mexico, and parts of Montana (see Figures 2a,3a). Subsidence was indicated behind the trough. Six-hourly satellite photos (SP) Figures 4a-c centered at the time of the VMF analysis, show middle-level clouds extending from central Idaho eastward into Montana and the Dakotas. These clouds were associated with a combination of weak UVV and low-level upslope flow east of the Divide in Montana. A surface high centered over northern Montana provided weak upslope winds enhancing precipitation in Montana and Wyoming. Convective activity occcurred throughout the day in Wyoming, Colorado, and New Mexico, in agreement with the weak UVV diagnosed. Comparison of Figure 3a with SP's 4a-c shows that areas of cloud development were in fair agreement with the diagnosed VMF. The area of maximum UVV appears fairly cloud-free in the satellite picture. However, the atmosphere was extremely dry at all levels in this area such that the large UVV had not yet brought the atmosphere to saturation. The UVV was evidenced however by a decrease in Boise's lifted index from 7 to 0 during the period from 12Z on the 19th to 00Z on the 20th. Also, since orographic vertical motion is not included in the physics of the diagnostic model, it did not indicate the cloudiness in eastern Montana and Wyoming or precipitation in southern Canada. On the positive side, note particularly in SP 4b (time coincident with VMF analysis) the cloud development in southwest Montana associated with the UVV maximum. Also note the cloud-free areas in the western half of the region in agreement with subsidence indicated by the VMF analysis.

By 12Z on the 20th the upper-level trough had moved southeastward with the trough axis extending from San Francisco, northeast to central Idaho. Figure 3b shows that the UVV maximum ($\geq$+1 cm sec^{-1}) had decreased slightly and moved eastward over the Idaho-Wyoming border. The overall character of the VMF did not change however. Weak UVV continued in the eastern part of the region ahead of the trough with subsidence in the west. Comparison of Figure 3b with SP's 4c-e shows continuing middle cloud development over eastern Idaho and Montana in the UVV area. However, SP 4e shows convective clouds forming over Montana and along the Idaho-Montana border near the UVV maximum.

By 00Z on the 21st the trough axis extended northeastward from central California to southeastern Idaho. The diagnosed area of rising motion ahead of the trough moved eastward into Wyoming, Utah, Colorado, central Arizona, and New Mexico. By this time southeastern Idaho, southwestern Montana, northern Utah, and western Wyoming had been in an area of UVV for at least 24 hours. Although the atmosphere was very dry, the prolonged UVV aided by diabatic (surface) heating during the day decreased atmospheric stability. Convective activity developed throughout the day and by 00Z well developed Cu and Cb clouds covered southeastern Idaho, southwestern Montana, northern Utah, Wyoming, and Colorado (see SP 4f). Precipitation resulting from this instability was light due to the dry low levels of the atmosphere. However, strong, gusty winds were reported with these storms. While UVV and precipitation occurred east of the trough, subsidence in the west continued to increase and reached diagnosed values of -2 cm sec^{-1} in eastern Oregon and Nevada. SP 4f shows the cloud-free area in the western half of the region.

The trough continued moving eastward and by 12Z on the 21st the axis extended from southeastern Arizona to western Wyoming (see Figure 2d). Figure 3d shows large areas of weak subsidence west of the trough. An area of UVV ($\leq$+1 cm sec^{-1}) was diagnosed in western Wyoming and Montana. SP 4h (12Z on the 21st) shows a small area of Cu remaining from the previous evening over Wyoming. Precipitation measuring up to .05 in fell in central Wyoming during the following 6 hours.

For the 36-hour summer case 00Z 7-20-78 to 12Z 7-21-78, a general trend of UVV ahead of the trough and weak subsidence following the trough were diagnosed. Cloud development occurred in areas ahead of the trough where diagnosed weak UVV was more prolonged, in agreement with the model. Scattered precipitation throughout Montana and Wyoming coincided with diagnosed UVV and low-level upslope flow east of the Divide. This case also illustrates that a prolonged period of UVV may be necessary to initiate precipitation in a dry atmosphere. Thus, the diagnostic system produced a realistic vertical-motion field that showed strong correlation with the atmosphere.

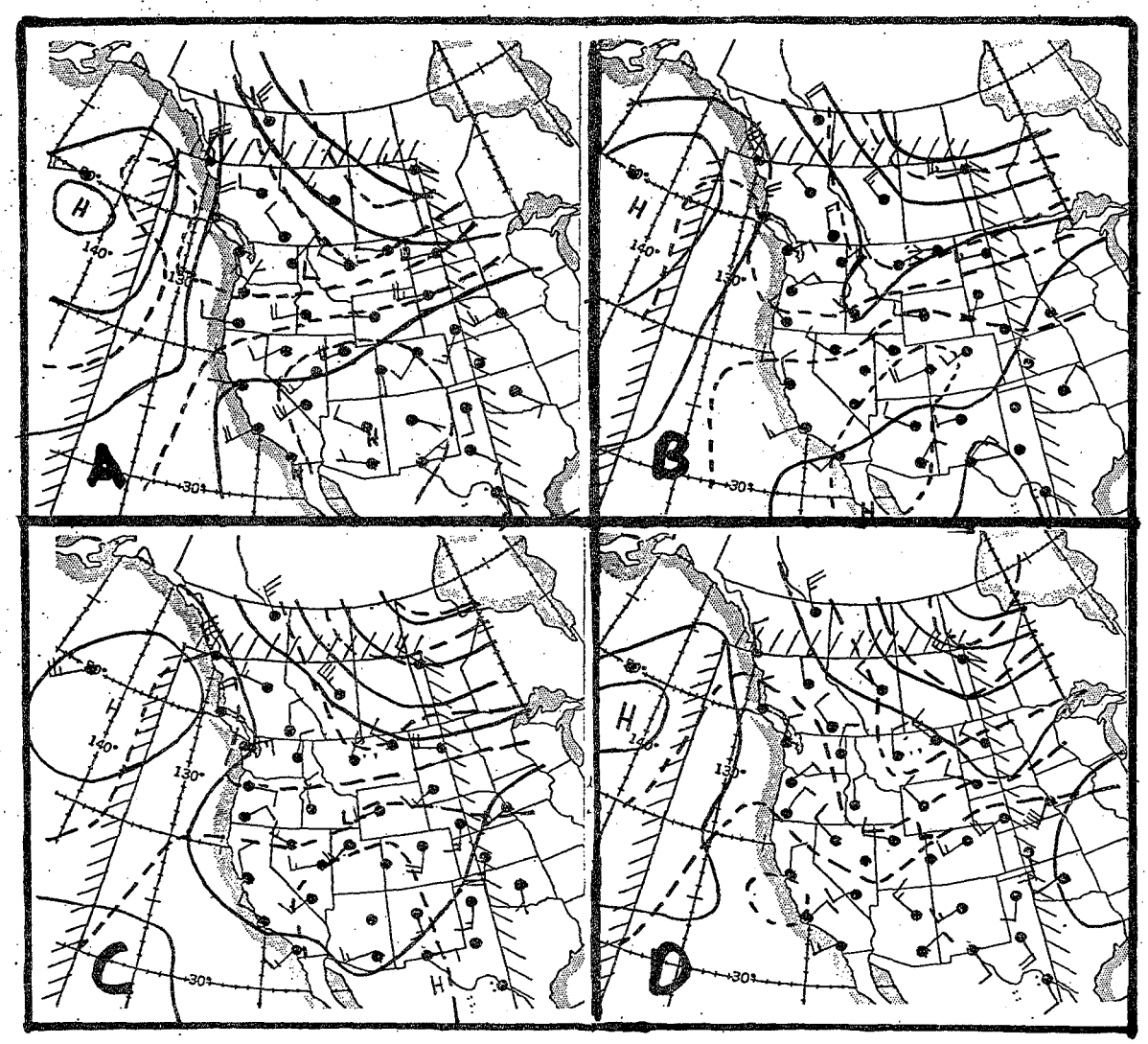

FIGURE 2A-D. 700-MB ANALYSIS VALID A) 00Z JULY 20, B) 12Z JULY 20, C) 00Z JULY 21, AND D) 12Z JULY 21. SOLID LINES ARE HEIGHT CONTOURS WITH AN INTERVAL OF 60 METERS. DASHED LINES ARE TEMPERATURE FIELD WITH CONTOUR INTERVAL OF 5°C.

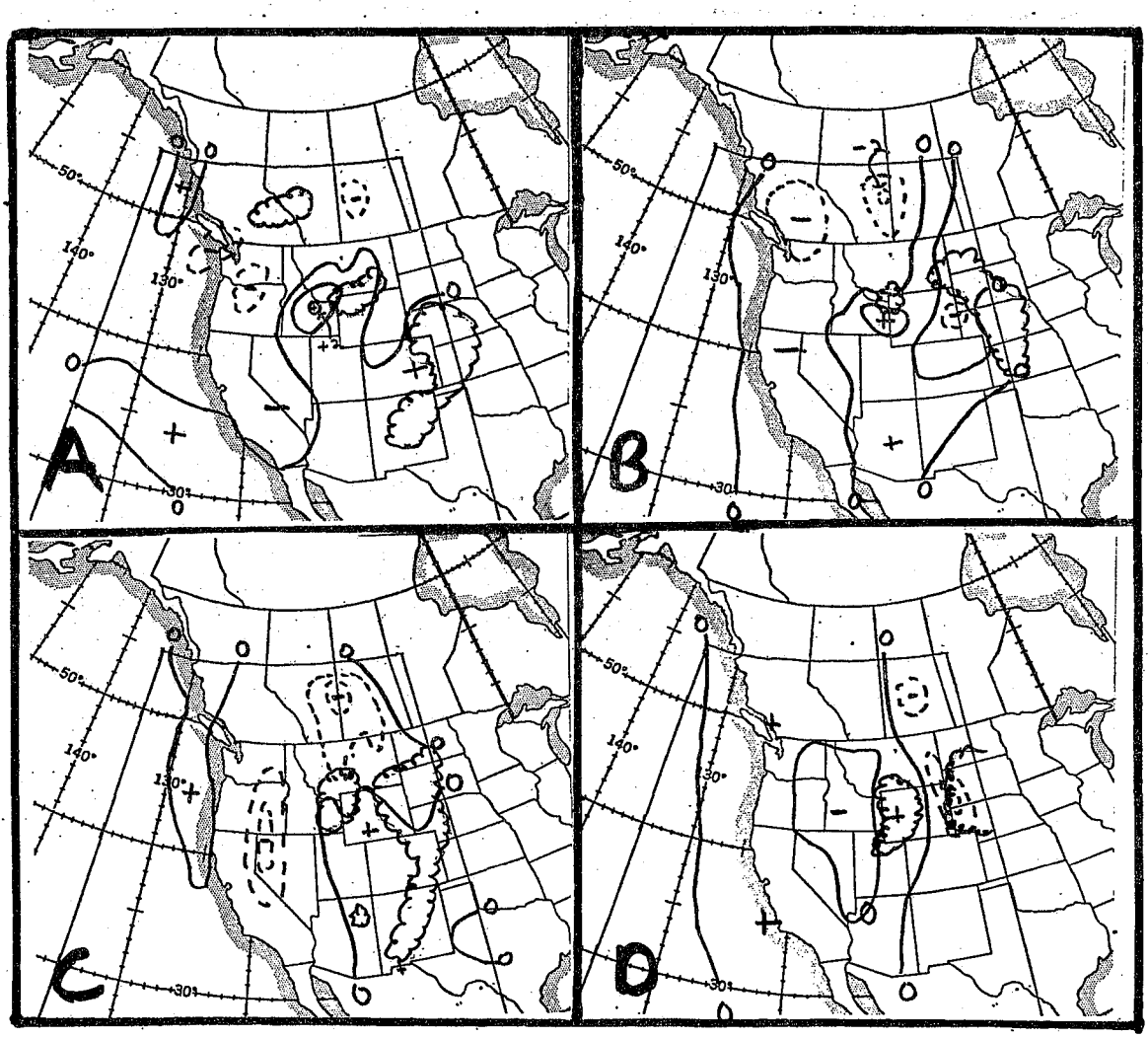

FIGURE 3A-D. DIAGNOSED VERTICAL MOTION VALID A) 00Z JULY 20, B) 12Z JULY 20, C) 00Z JULY 21, AND D) 12Z JULY 21. THE CONTOUR INTERVAL IS 1 CM/SEC WITH DASHED CONTOURS INDICATING SINKING MOTION. THE SCALLOPED AREA OUTLINES AREAS OF PRECIPITATION FOR THE 12-HOUR PERIOD CENTERED ON THE TIME OF THE VERTICAL-MOTION FIELD.

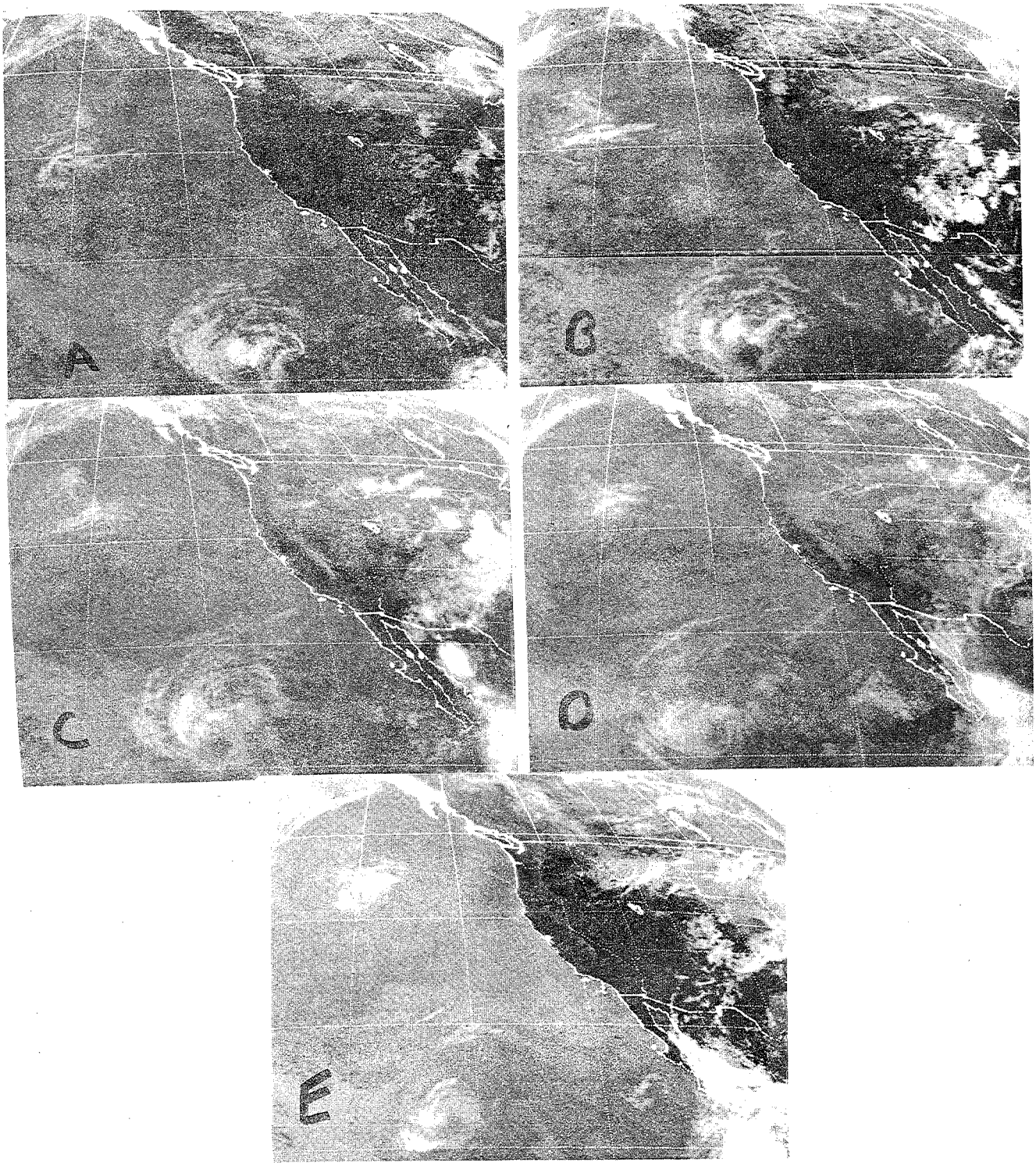

FIGURE 4A-E. IR SATELLITE PHOTOS FROM A) 1745Z JULY 19, B) 2345Z JULY 19, C) 0545Z JULY 20, D) 1145Z JULY 20 AND E) 1745Z JULY 20.

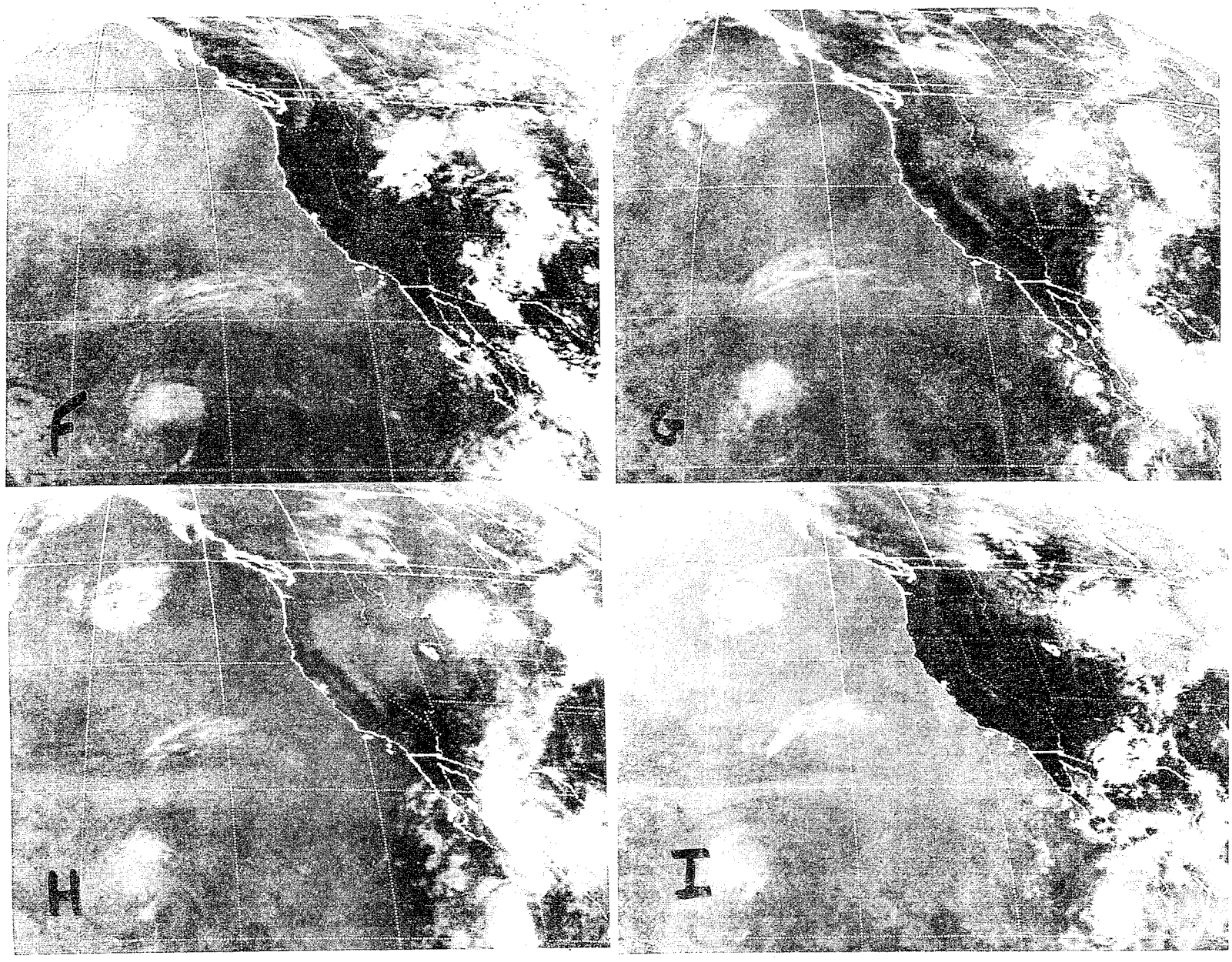

FIGURE 4F-I. IR SATELLITE PHOTOS FROM F) 2345Z JULY 20, G) 0545Z JULY 21, H) 1145Z JULY 21, AND I) 1745Z JULY 21.

b. April 7 - 8, 1978

On 00Z April 7, 1978, an upper-level trough was centered over northern California. During the next 24 hours, this intense system moved southeastward digging into southern Nevada (see Figures 5a-c). At the surface a cold front extended from northwestern Montana southeastward along the Divide into northeastern Wyoming. By 12Z on the 7th the front became stationary along the Idaho-Montana border into central Wyoming. A second cold front extended from central Idaho southwestward through central Nevada, to near Los Angeles. The front had become quasi-stationary. A vigorous vorticity maximum dropped down the back side of the trough and initiated a frontal wave that moved progressively eastward and by 00Z on the 8th was located in Utah and central Arizona. Precipitation occurred throughout most of the western United States with heaviest amounts in California, Nevada and Idaho.

Figure 6a shows the VMF analysis for 00Z on the 7th. Maximum UVV of γ+1 cm sec^{-1} was diagnosed throughout Idaho, Montana, northern Utah, and western Wyoming. This would appear to be associated with the strong warm advection in this area. Maximum subsidence areas were diagnosed off the Oregon coast, in southwest Colorado, and central California. Six hourly satellite photos, Figures 7a-c, show middle-level and high-level clouds over most of the region. Strong warm-air advection over Utah, Idaho, western Oregon, and Montana resulted in cloud formation and precipitation coincident with the diagnosed UVV. The convection associated with the vorticity maximum and cold air over northern California is not indicated to have strong UVV. This may be partly due to the fact that diabatic effects are not contained in the model. No cloud development occurred in diagnosed subsidence areas north of the U. S.-Canadian border and off the Oregon-Washington coast where a high-pressure ridge extended southwest from Vancouver Island. Subsidence diagnosed at the Four Corners is evidenced by clear skies in Arizona, New Mexico, and southwest Colorado during the 6 hours following the VMF analysis (see SP's 7b,c). Subsidence (γ-1 cm sec^{-1}) was diagnosed throughout most of California and Nevada, but surface data indicated significant precipitation with the cold front which was located in central California and Nevada.

It appears the model did not verify well in this area since weak subsidence was diagnosed with the strong cold advection indicated on the 700-mb analysis. However, careful comparison of the satellite data and the analysis indicated that the analysis over southern California and offshore was quite poor. The 700-mb height and wind at Oakland did not

seem to fit the other data. Also, satellite data indicated a rather sharp trough to be off the coast while the analysis showed weak cyclonic curvature. Using a careful reanalysis and bogus data, a much more satisfactory initial analysis was obtained (Figure 5d). The recomputed vertical motion field indicated rising motion of greater than 71 cm/sec throughout central California and Nevada. This indicates that careful attention must be paid to bogusing systems in data-sparse areas.

The LFM-II 12-hour prognostic vertical motion field valid at 00Z on the 7th is shown in Figure 8a. It indicated rising motion over almost the whole western United States with strong rising motion over northern California. The resolution of the diagnosed field makes it superior to this rather general prognostic field.

By 12Z on the 7th the vort max and cold air were digging into central California. The trough that had been off the coast had weakened and moved northeastward into Utah and Nevada. Warm advection continued over the northeast quadrant of the western United States. The California cold front had moved southeastward extending from San Diego northeastward along the Nevada-Utah border into central Wyoming. Figure 6b shows the VMF analysis for 12Z. UVV was diagnosed along a northeast-southwest axis covering central California, Nevada, Idaho, western Wyoming, and Montana. Maximum UVV of greater than +2 cm sec^{-1} was diagnosed in central Nevada and north-central Montana. Subsidence was diagnosed east and west of the UVV zone, with maximum values of -3 cm sec^{-1} in Arizona and the Four Corners area. Six-hourly satellite photos, Figures 7c-e, show good agreement of cloud development with the VMF analysis. SP 7d, taken at the time of the VMF analysis, shows clouds covering Nevada, southern Idaho, and northwest Utah in the diagnosed UVV area behind the front. At the surface, light to moderate snow was falling in central Nevada in excellent agreement with the diagnosed UVV. This would appear to be associated with the weakening vort max moving northeastward. Middle clouds covered northern Idaho and Montana where maximum UVV was diagnosed as strong warm-air advection continued. Cloud development also occurred in the UVV area off the southern California coast with the vorticity maximum. This again was handled only marginally well.

Arizona, New Mexico, and Colorado were located in diagnosed maximum subsidence areas and are shown to be generally cloud-free (see SP 7d). Some orographic cloud development not taken into account by the model did occur along the Colorado-Utah border, however. Also cloud-free is the diagnosed subsidence area off the coast associated with the high-pressure ridge west of the trough.

The LFM 12-hour vertical-motion prog is shown in Figure 8b. It shows maximum rising motion in central Arizona and also off the California coast. It fails to show the strong rising motion in central Nevada and would appear to have an incorrect sign in Arizona. The diagnosed pattern is far superior.

By 00Z on the 8th the trough was centered over central Nevada. The California cold front extended from eastern Utah through Arizona into Baja California. The Montana front remained stationary along the Idaho-Montana border and through central Wyoming. Figures 5c and 6c show the 700-mb and VMF analysis at 00Z, respectively. The overall pattern of the VMF did not change in the 12-hour period. However, diagnosed UVV now covers all of Oregon and all but northwest Washington. Diagnosed UVV increased to +2 cm sec^{-1} in eastern Oregon. Maximum UVV in central Montana and off the southern California coast continued to be associated with strong warm-air advection and the vorticity maximum, respectively.

Diagnosed subsidence continued throughout the Four Corners states with values increasing to -4 cm sec^{-1} in central Arizona. Subsidence also continued off the coast as the high-pressure ridge intensified and moved into the area.

SP 7f taken at the time of the VMF analysis (00Z on the 8th) shows low- and middle-level clouds in the diagnosed UVV area (Nevada, Oregon, Washington, Idaho, Montana, and Utah). Scattered, light precipitation was recorded throughout Nevada, Utah, and Idaho. The Four Corners/Arizona area was clearer than the rest of the region. Although some light precipitation fell in the Flagstaff, Arizona, area with the cold front.

SP 7f shows thin, scattered, low- and high-level clouds off the coast in the diagnosed subsidence area 132W/30-45N. The diagnosed strong subsidence (-6 cm sec^{-1}) resulted in dissipation of clouds in the hours following the VMF analysis (see SP 7g). Dissipation continued as new clouds entered the area around the high-pressure ridge to the northwest.

Figure 8c shows the LFM-II 12-hour prognostic VMF. The rising motion it indicates in Arizona resulted in light precipitation. The main activity, as diagnosed, was occurring farther north.

The diagnosed VMF appears to be in good agreement with both UVV and subsidence areas which developed during the winter case 00Z on the 7th

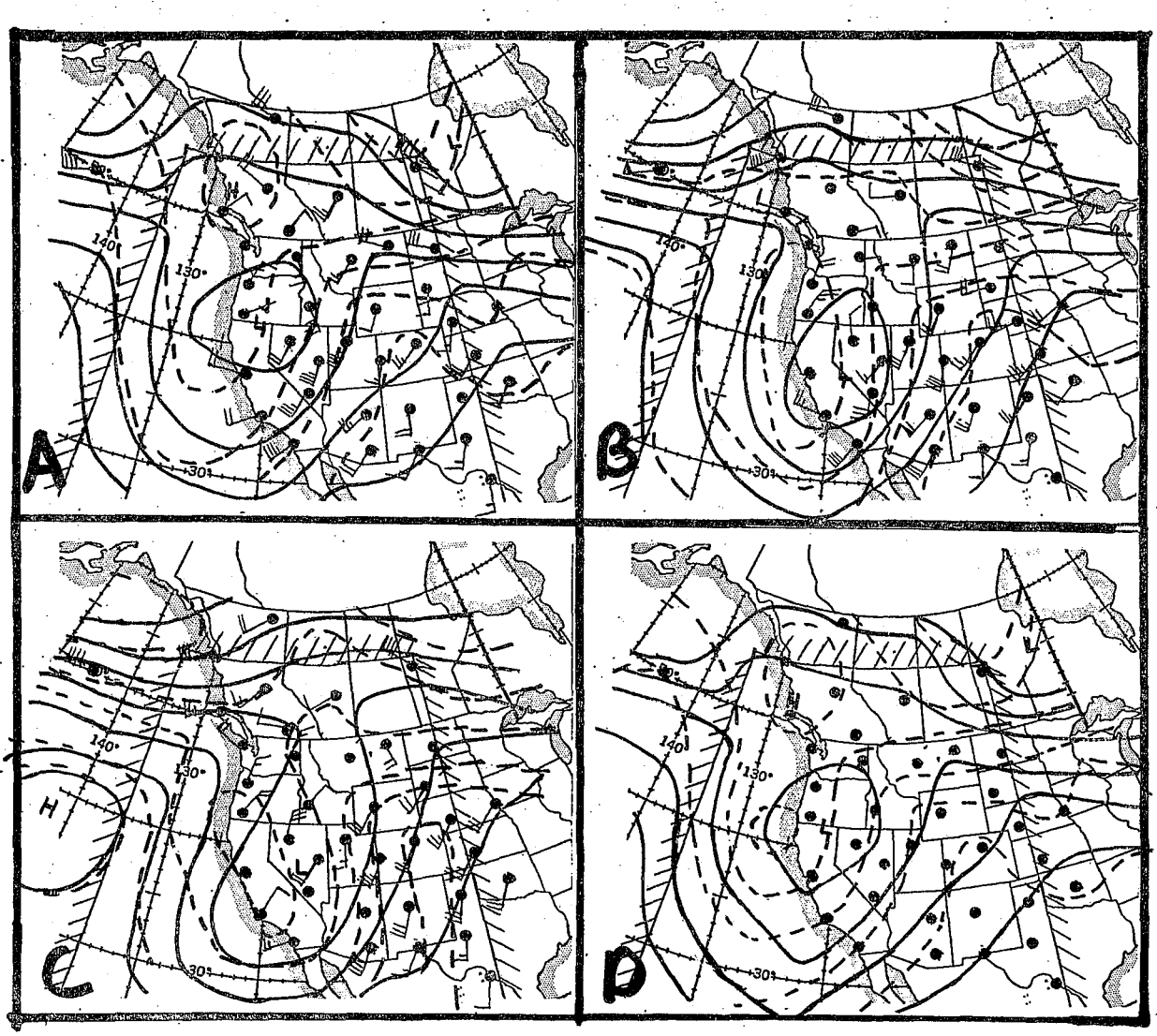

FIGURE 5A-D. 700-MB ANALYSIS VALID A) 00Z APRIL 7, B) 12Z APRIL 7, C) 00Z APRIL 8, AND D) 00Z APRIL 7 REANALYZED.

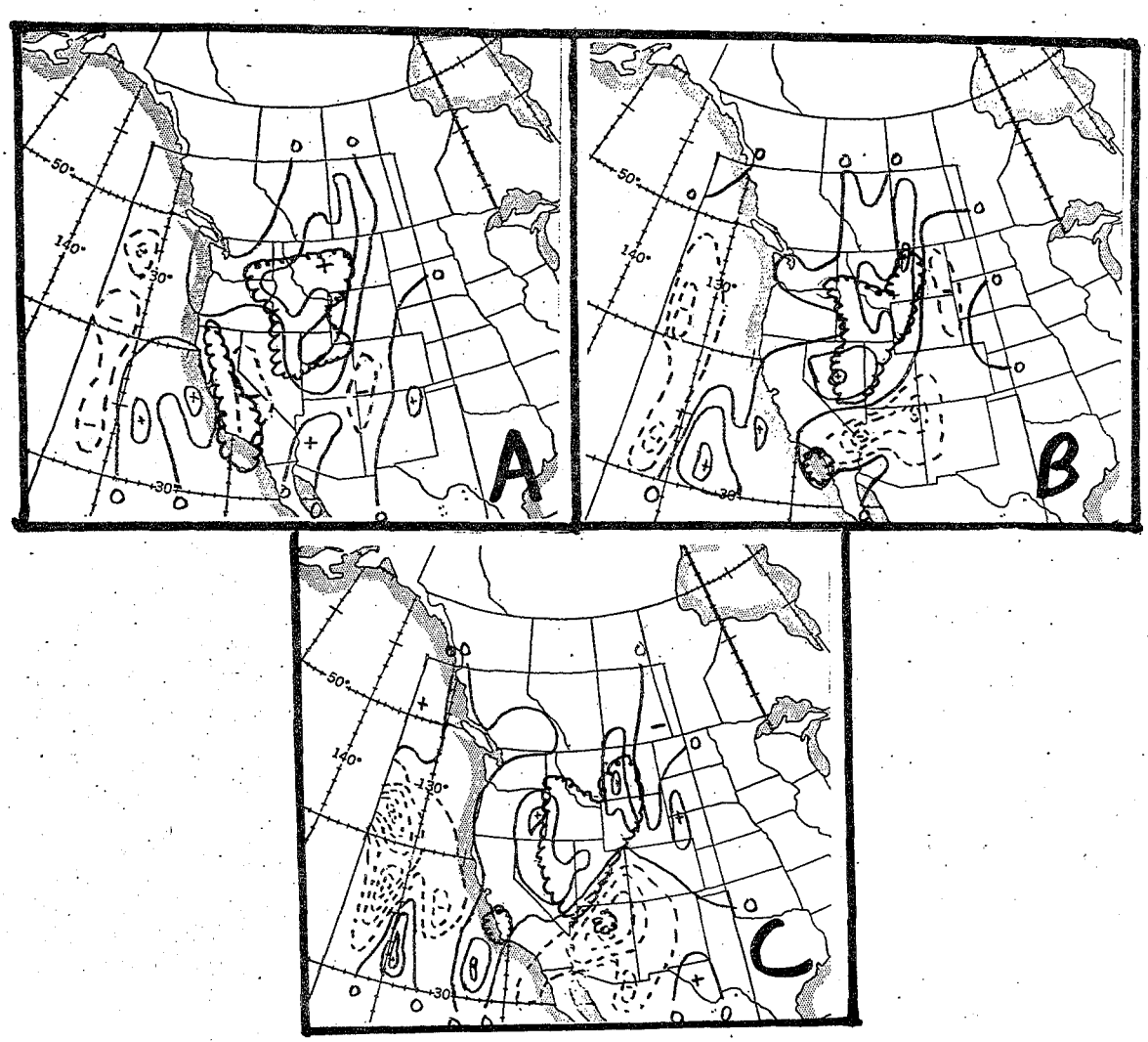

FIGURE 6A-C. DIAGNOSED VERTICAL MOTION AND PRECIPITATION VALID A) 00Z APRIL 7, B) 12Z APRIL 7, AND C) 00Z APRIL 8.

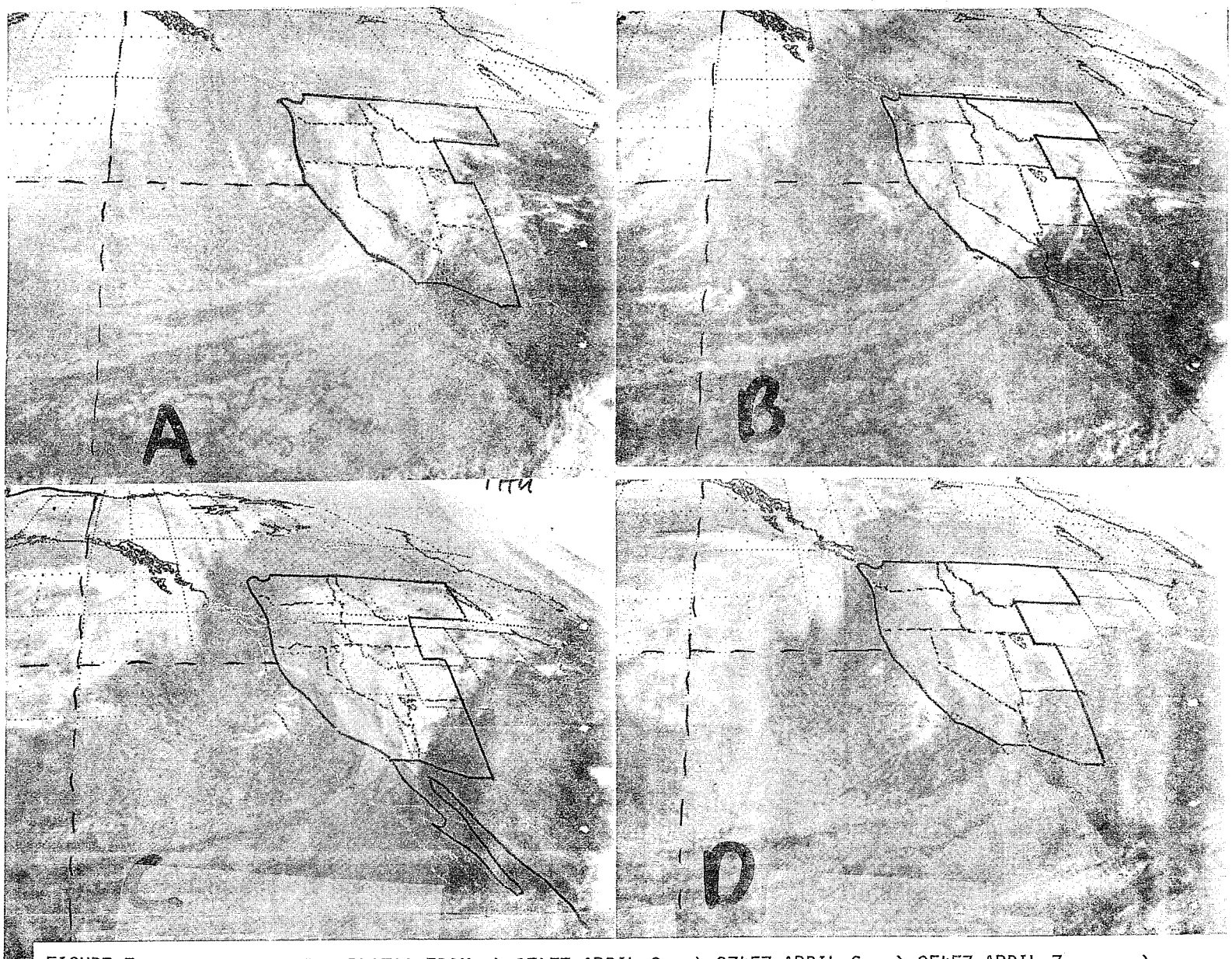

FIGURE 7A-D. IR SATELLITE PHOTOS FROM A) 1745Z APRIL 6, B) 2345Z APRIL 6, C) 0545Z APRIL 7, AND D) 1145Z APRIL 7. THE ORIGINAL GRID ON 7c WAS CONSIDERABLY OFF; OVERDRAWN GRID IS APPROXIMATELY CORRECT.

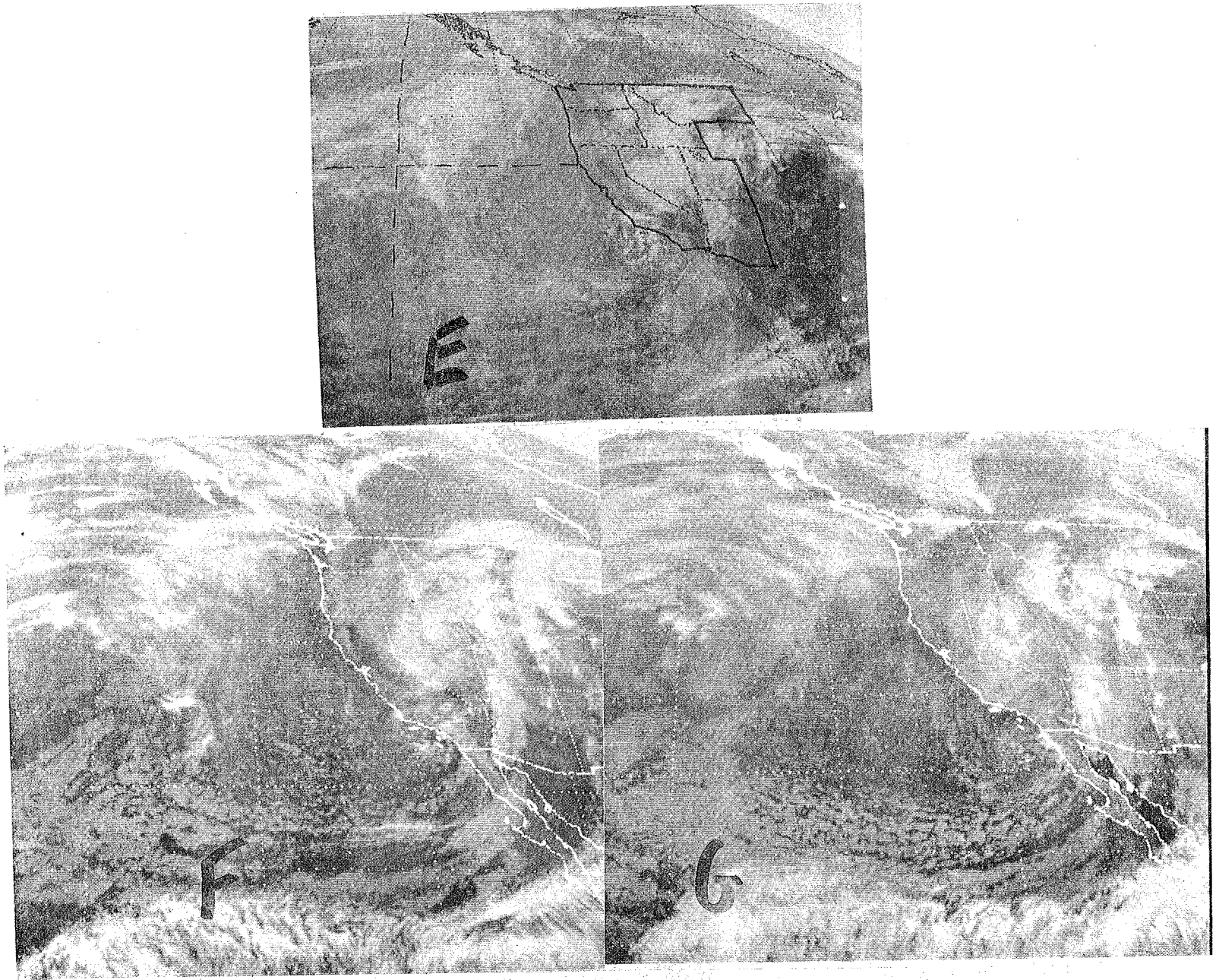

FIGURE 7E-G. IR SATELLITE PHOTOS FROM E) 1745Z APRIL 7, F) 0145Z APRIL 8, AND G) 0745Z APRIL 8.

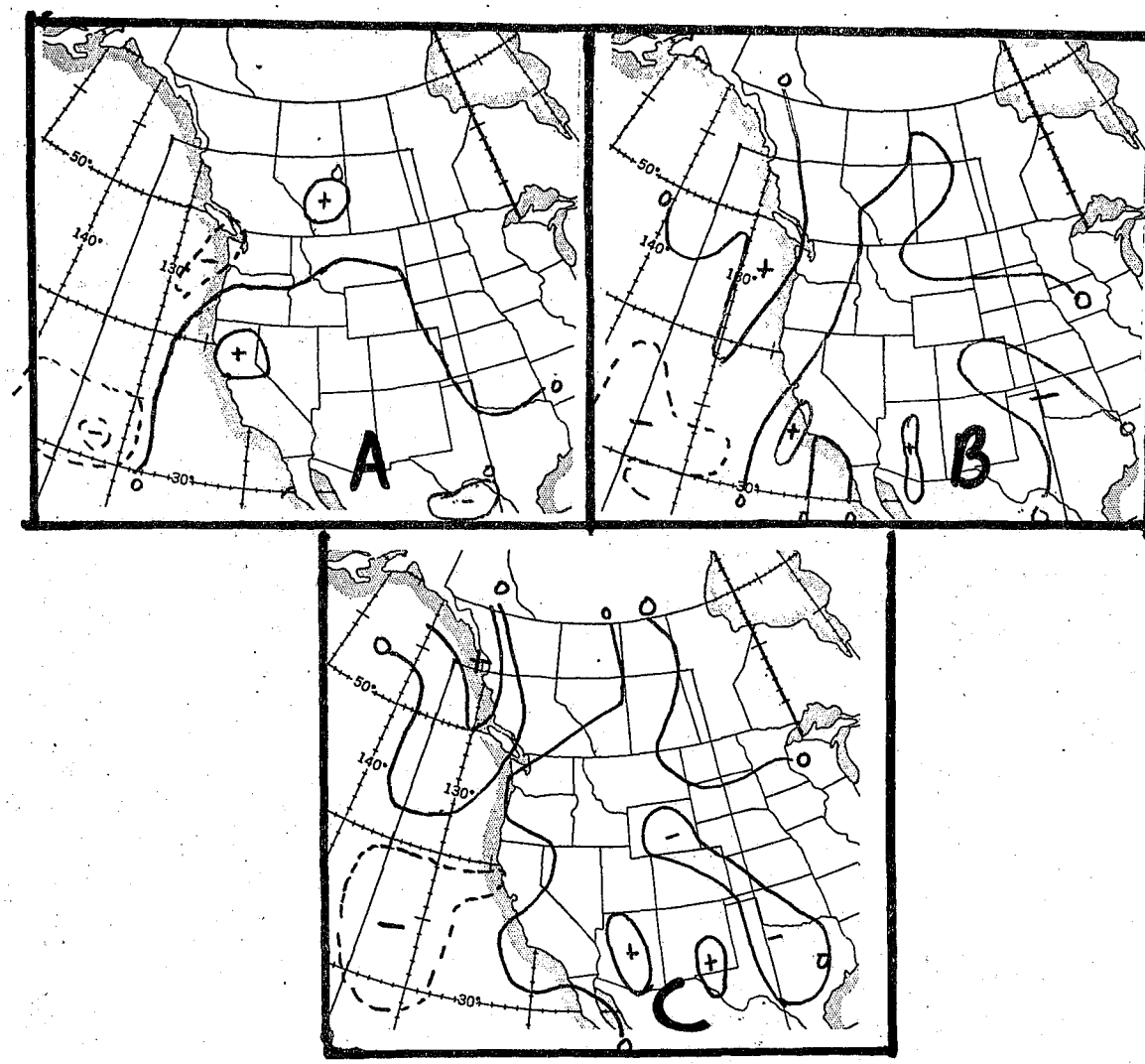

FIGURE 8A-C. LFM-II 12-HOUR 700-MB VERTICAL VELOCITY PROG VALID A) 00Z APRIL 7, B) 12Z APRIL 7, AND C) 00Z APRIL 8. CONTOUR INTERVAL IS 2 MICROBARS/SECOND WITH DASHED CONTOURS INDICATING SINKING MOTION.

to 00Z on the 8th of April 1978. With the exception of weak subsidence diagnosed behind the California cold front on the 7th, diagnosed UVV areas were in good agreement with observed precipitation and cloud coverage. The model successfully diagnosed UVV in areas of strong warm-air advection and maximum vorticity. Areas of downward vertical motion also seem to verify well. This case strongly emphasizes the need for a good analysis in data-sparse areas in order to obtain satisfactory results.

c. June 25, 1978

On 00Z June 25, 1978, an upper-level trough was centered over the northwestern United States (Figure 9). Figure 10 and SP 11 show the diagnosed VMF and satellite photo at 00Z on the 25th, respectively. Vigorous convective activity occurred in southeastern Idaho, Wyoming, northeastern Utah, and Montana in the diagnosed UVV area ahead of the trough. Well-developed thunderstorms occurred in Montana coincident with the UVV maximum ($+1.6$cm sec^{-1}). Heaviest precipitation occurred in central Montana with amounts measuring up to .49 inch. Scattered precipitation occurred in central Oregon, southeastern Washington, Idaho, and Montana in the six hours preceding the VMF analysis. Middle-level clouds can be seen in the diagnosed subsidence area over Oregon. This area of sinking was caused by an erroneous short-wave ridge analyzed in the 700-mb height field by the objective technique. Strong subsidence was indicated in the cold advection area over Nevada and California. This is in good agreement with Figure 11.

The LFM-II 12-hour prognostic VMF valid at the same time is shown in Figure 12. It indicated weak subsidence in the southwestern United States and northeastern Montana with weak UVV elsewhere. The area of subsidence in Montana is where the heaviest precipitation occurred. It does indicate the UVV and precipitation that occurred in Oregon.

In this case, UVV diagnosed ahead of the trough aided strong diabatic heating and was associated with thunderstorm activity in the northeastern part of the Region. No clouds occurred in California, Arizona, or Nevada in the area of diagnosed subsidence (-3cm sec^{-1}). In this case, the model diagnosed VMF seems to be in good agreement with vertical motion implied by the atmosphere.

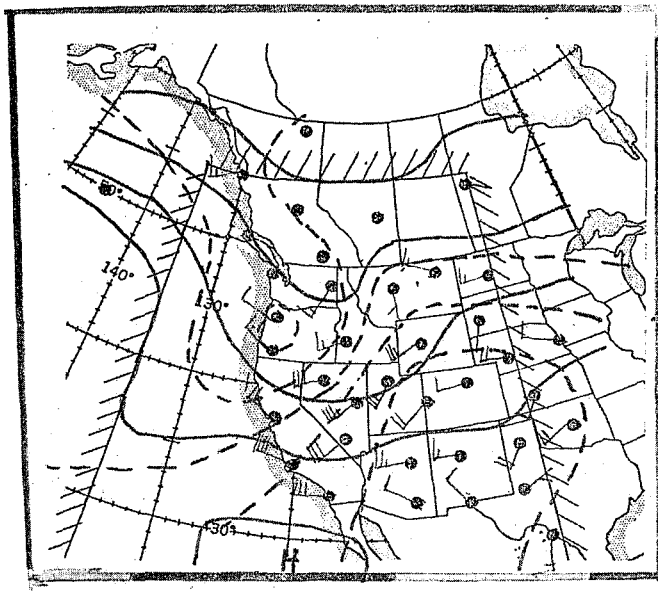

FIGURE 9. 700-MB ANALYSIS VALID 00Z JUNE 25.

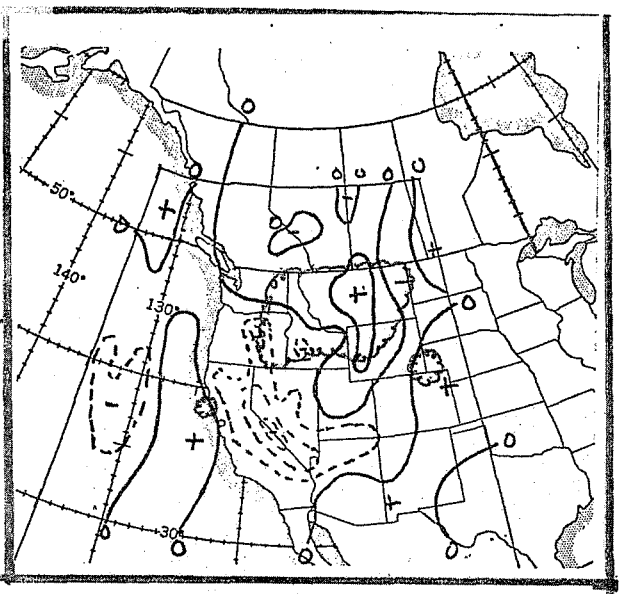

FIGURE 10. DIAGNOSED VERTICAL MOTION AND PRECIPITATION VALID 00Z JUNE 25.

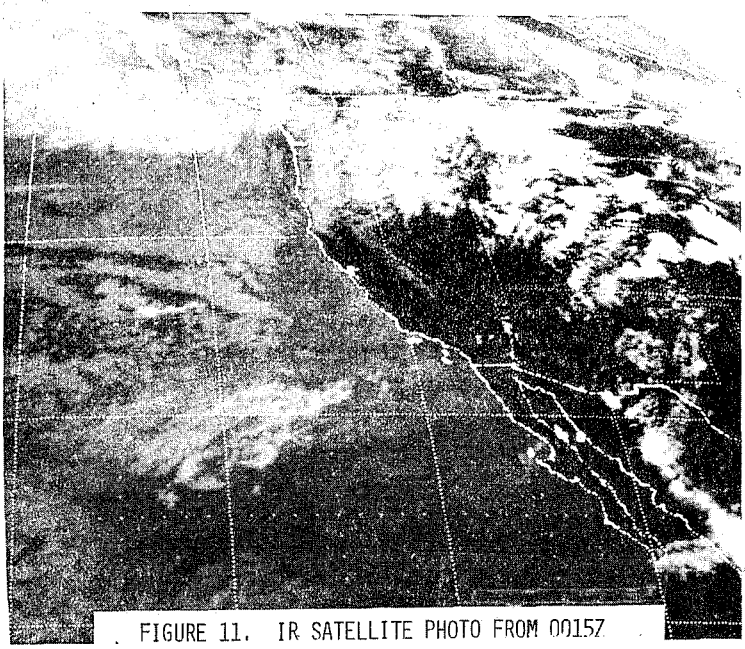

FIGURE 11. IR SATELLITE PHOTO FROM 0015Z JUNE 25.

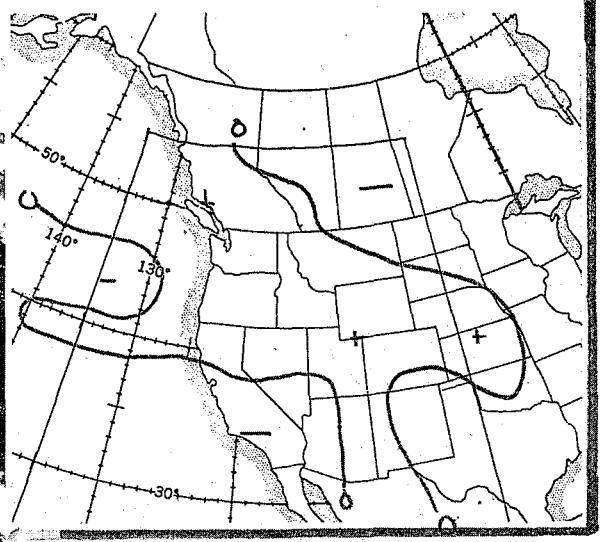

FIGURE 12. LFM-II 12-HR 700-MB VERTICAL VELOCITY PROG VALID 00Z JUNE 25.

[9] Panofsky, H. A., 1946: Methods of Computing Vertical Motion in the Atmosphere. Journal of Meteorology, 3, 45-49.

[10] Petterssen, S., 1955: A General Survey of Factors Influencing Development at Sea Level. Journal of Meteorology, 12, 36-42.

[11] Stuart, D. W., 1964: A Diagnostic Case Study of the Synoptic Scale Vertical Motion and Its Contribution to Mid-Tropospheric Development. Journal of Applied Meteorology, 3, 669-684.

[12] Sutcliffe, R. C., 1947: A Contribution to the Problem of Development. Quarterly Journal Royal Meteorological Society, 73, 370-383.

[13] Trenberth, K. E., 1978: On the Interpretation of the Diagnostic Quasi-Geostrophic Omega Equation. Monthly Weather Review, 106, 131-137.

[14] Whittaker, T. M., 1976: A Simplified Grid Interpolation Scheme for Use in Atmospheric Budget Studies. Masters Thesis, University of Wisconsin, Madison, Wisconsin, 42 pp.

Another use of this field would be in evaluating the initial analysis for the operational numerical weather prediction models. This point was illustrated in the April case. In that case, even though the objective analysis was in close agreement with the LFM-II initial analysis, the diagnosed vertical-motion field was quite poor. Careful reanalysis of the height and temperature fields offshore using satellite data provided a quite reasonable vertical-motion field. Thus, by comparing the diagnosed vertical-motion field and the satellite picture, one may get a good handle on the quality of the initial analysis for the NWP models.

Certainly this model has many other uses, but it also has some limitations. The main limitations are that the quasigeostrophic w-equation neglects terrain effects and diabatic effects. Both of these can be important in forecasting the weather for a given locale. Terrain effects could be added to this model with little increase in computer time.

V. CONCLUSION

The diagnostic VMF computed using Hoskins' [6] one-level omega equation appeared to be in good agreement with areas of cloud development and subsidence which occurred in the atmosphere, associated with large-scale midlatitude synoptic systems in the cases studied. Areas of UVV diagnosed by the VMF model correlated well with cloud coverage and precipitation; also, cloud-free areas were in good agreement with subsidence diagnosed by the model. Clouds located in diagnosed subsidence areas at the time of the VMF analysis, showed a decreasing trend as dispersion continued in the hours following the analysis. It is clear that the VMF model gave better estimates of vertical motion with better resolution and well-defined boundaries than is available on the LFM prognostic charts.

On the other hand weak, small-scale features were overly smoothed by the objective analysis and gave poor results for the diagnosed VMF. When small-scale features are indicatd on time coincident satellite photos or poorly analyzed small-scale features are suspected on the NMC 700-mb analysis, extensive bogusing of data and reanalysis may increase the accuracy of the diagnosed VMF. Also, poor results may be obtained when the significant synoptic feature falls in a data-sparse area. Careful use of satellite data and bogusing can give good results however.

The VMF model described here can easily be modified for use in any geographic area by simply changing the grid boundaries and latitude and longitude of the data points to be entered. Through the use of the diagnostic VMF model, the forecaster has available both qualitative and quantitative information based on real-time upper-level analyses to assist in precipitation forecasting.

VI. ACKNOWLEDGMENTS

The authors would like to thank the staff of Scientific Services Division (SSD), National Weather Service, Western Region Headquarters, whose patience and helpful suggestions made the writing of this paper possible. Especially Evelyn Allan for her typing and retyping of this manuscript. Also the help of the San Francisco Satellite Field Services Station in providing satellite data is appreciated.

VII. REFERENCES

[1] Astling, E. G., 1976: Some Aspects of Cloud and Precipitation Features Associated with a Mid-latitude Cyclone. Monthly Weather Review, 104, 1466-1473.

[2] Cooley, D. S., 1978: High Resolution LFM (LFM-II). Technical Procedures Bulletin No. 206, Technical Procedures Branch, NOAA, U. S. Dept. Commerce, Silver Spring, Maryland, 6 pp.

[3] Cressman, G. P., 1954: An Approximate Method of Divergence Measurement. Journal of Meteorology, 11, 83-90.

[4] Cressman, G. P., 1959: An Operational Objective Analysis System. Monthly Weather Review, 87, 367-374.

[5] Haltiner, G. J., 1971: Numerical Weather Prediction, John Wiley and Sons, Inc., 317 pp.

[6] Hoskins, B. J.; I. Draghici, and H. C. Davies, 1978: A New Look at the W-Equation. Quarterly Journal Royal Meteorological Society, 104, 31-38.

[7] Krishnamurti, T. N., 1968: Diagnostic Balance Model for Studies of Weather Systems of Low and High Latitudes, Rossby Number Less Than 1. Monthly Weather Review, 4, 197-207.

[8] Krisnamurti, T. N., 1968: A Study of a Developing Wave Cyclone. Monthly Weather Review, 96, 208-217.

d. July 26, 1978

12Z July 26, 1978, the 700-mb analysis showed a high-pressure center over Nevada and Utah. The NMC 700-mb analysis showed no perturbations in height contours south of the high center (Figure 13). The analysis did show a weak trough off the coast at 135W/40-53N. Figure 14 shows the VMF obtained using the above 700-mb data. Weak subsidence was diagnosed in the southwest part of the region (< -1cm sec^{-1}) with weak UVV diagnosed over Oregon, Washington, and Idaho ($< +1$cm sec^{-1}). Satellite data from the time of the VMF analysis (12Z on the 26th, Figure 15) shows convective activity in southwest Arizona and middle-level clouds covering much of northern California, western Nevada, Oregon, and Washington. There also appeared to be two vorticity maxima indicated; one in southwestern Arizona and another on the Nevada-California border. The VMF did not diagnose significant UVV in these areas. Reanalysis of the 700-mb data using the satellite picture confirmed the two vorticity maxima. Also, the trough off the coast was deepened by reanalysis. The VMF was recomputed with some bogusing of the vorticity centers attempted. However, the VMF was changed only slightly.

The poorer results obtained by the VMF for this case seem to be due to poor analysis of weak, small-scale features at the 700-mb level, rather than some fault in the vertical-motion model.

Any type of scan analysis will give some smoothing of small-scale features. Thus, unless small-scale features are heavily bogused, the analysis routine will smooth them and yield a bland vertical-motion field. This is not a serious problem for typical synoptic scales but must be considered when using this type of analysis scheme.

IV. SYNOPTIC APPLICATIONS

This type of program has many applications to the operational forecaster. The most obvious application is in providing the forecaster with a real-time, detailed vertical-motion field. This would be invaluable in forecasting intensification and decay of systems. The whole process could be largely automated under the AFOS system. The upper-air data could be automatically accessed and the forecaster would only need to input a few bogus points. The analysis procedure takes about 6 minutes on an Eclipse S-230 minicomputer. Thus, with minimal effort the forecaster could have a detailed vertical-motion field shortly after the receipt of the upper-air data.

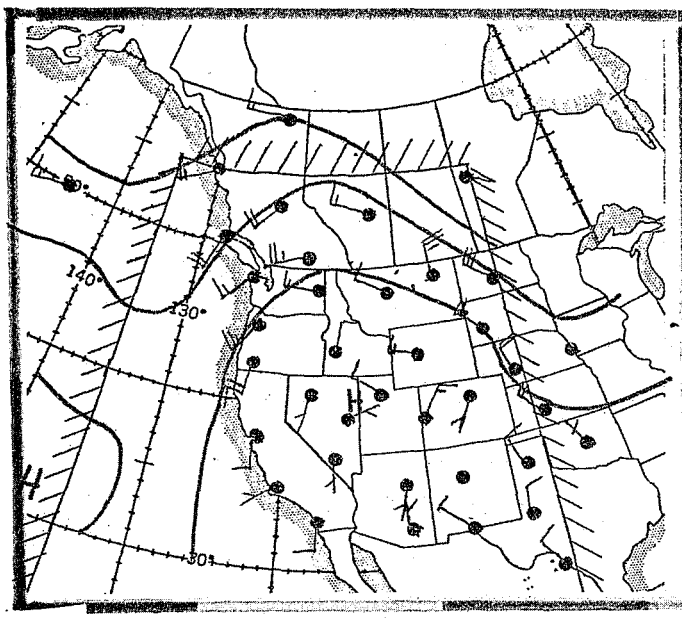

FIGURE 13. 700-MB ANALYSIS VALID 12Z JULY 26.

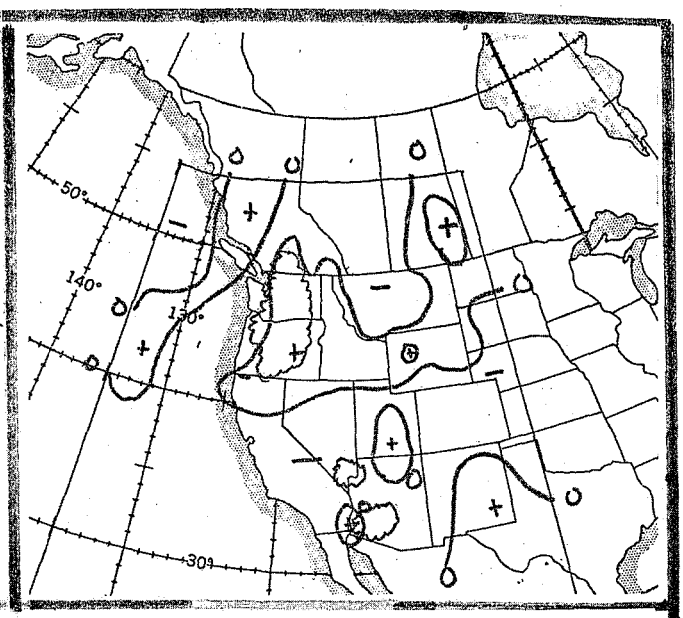

FIGURE 14. DIAGNOSED VERTICAL MOTION AND PRECIPITATION VALID 12Z JULY 26.

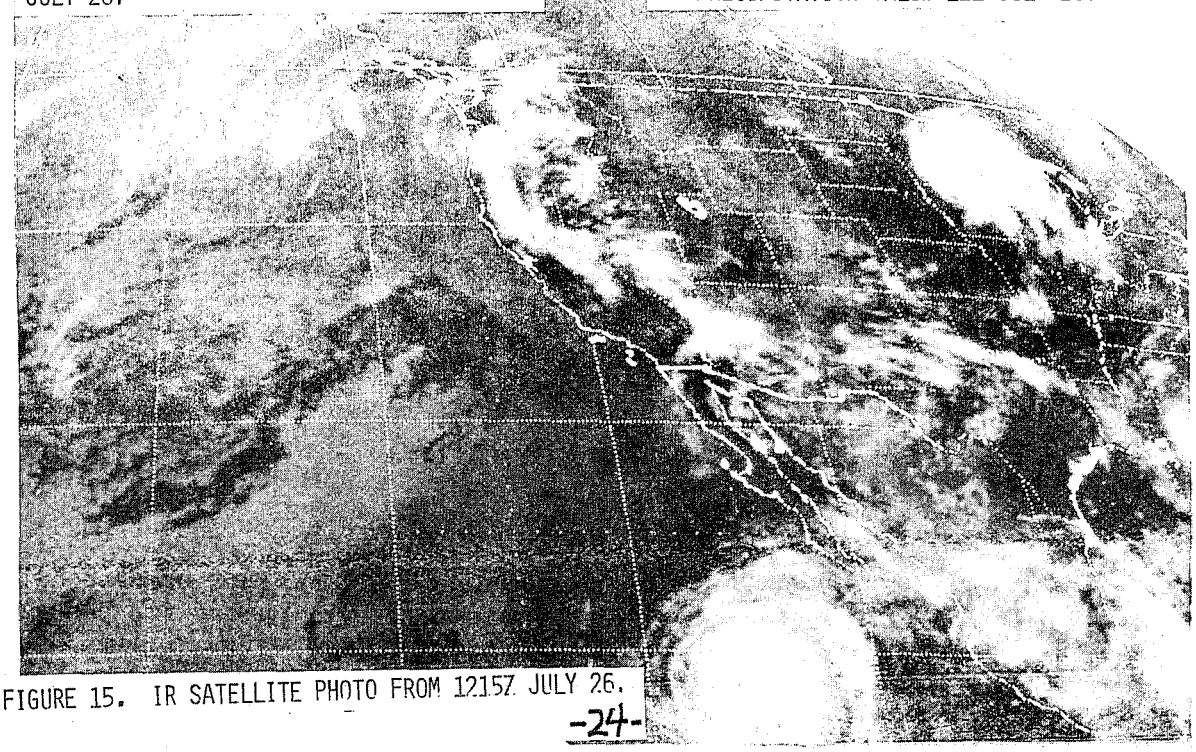

FIGURE 15. IR SATELLITE PHOTO FROM 1215Z JULY 26.

NOAA Technical Memoranda NWSWR: (Continued)

92 Smoke Management in the Willamette Valley. Earl M. Bates, May 1974. (COM-74-11277/AS)
93 An Operational Evaluation of 500-mb Type Stratified Regression Equations. Alexander E. MacDonald, June 1974. (COM-74-11497/AS)
94 Conditional Probability of Visibility Less than One-Half Mile in Radiation Fog at Fresno, California. John D. Thomas, August 1974. (COM-74-11555/AS)
95 Climate of Flagstaff, Arizona. Paul W. Sorenson, August 1974. (COM-74-11678/AS)
96 Map Type Precipitation Probabilities for the Western Region. Glenn E. Rasch and Alexander E. MacDonald, February 1975. (COM-75-10428/AS)
97 Eastern Pacific Cut-off Low of April 26-28, 1974. William J. Alder and George R. Miller, January 1976. (PB-250-711/AS)
98 Study on a Significant Precipitation Episode in the Western United States. Ira S. Brenner, April 1975.(COM-75-10719/AS)
99 A Study of Flash Flood Susceptibility--A Basin in Southern Arizona. Gerald Williams, August 1975. (COM-75-11360/AS)
100 A Study of Flash-Flood Occurrences at a Site Versus Over a Forecast Zone. Gerald Williams, Aug. 1975.(COM-75-11404/AS)
102 A Set of Rules for Forecasting Temperatures in Napa and Sonoma Counties. Wesley L. Tutt, Oct. 1975. (PB-246-902/AS)
105 Application of the National Weather Service Flash-Flood Program in the Western Region. Gerald Williams, January 1976. (PB-253-033/AS)
104 Objective Aids for Forecasting Minimum Temperatures at Reno, Nevada, During the Summer Months. Christopher D. Hill, January 1976. (PB-252-866/AS)
105 Forecasting the Mono Wind. Charles F. Ruscha, Jr., February 1976. (PB-254-650)
106 Use of MOS Forecast Parameters in Temperature Forecasting. John C. Plankinton, Jr., March 1976. (PB-254-649)
107 Map Types as Aid in Using MOS PoPs in Western United States. Ira S. Brenner, August 1976. (PB-259-594)
108 Other Kinds of Wind Shear. Christopher D. Hill, August 1976. (PB-260-457/AS) (PB-273-677/AS)
109 Forecasting North Winds in the Upper Sacramento Valley and Adjoining Forests. Christopher E. Fontana, Sept. 1976.
110 Cool Inflow as a Weakening Influence on Eastern Pacific Tropical Cyclones. William J. Denney, November 1976. (PB-264-635/AS)
112 The MAN/MOS Program. Alexander E. MacDonald, February 1977. (PB-265-941/AS)
113 Winter Season Minimum Temperature Formula for Bakersfield, California, Using Multiple Regression. Michael J. Oard, February 1977. (PB-273-694/AS)
114 Tropical Cyclone Kathleen. James R. Fors, February 1977. (PB-273-676/AS)
116 A Study of Wind Gusts on Lake Mead. Bradley Colman, April 1977. (PB-268-847)
117 The Relative Frequency of Cumulonimbus Clouds at the Nevada Test Site as a Function of K-value. R. F. Quiring, April 1977. (PB-272-851)
118 Moisture Distribution Modification by Upward Vertical Motion. Ira S. Brenner, April 1977. (PB-268-740)
119 Relative Frequency of Occurrence of Warm Season Echo Activity as a Function of Stability Indices Computed from the Yucca Flat, Nevada, Rawinsonde. Darryl Randerson, June 1977. (PB-271-290/AS)
121 Climatological Prediction of Cumulonimbus Clouds in the Vicinity of the Yucca Flat Weather Station. R. F. Quiring, June 1977. (PB-271-704/AS)
122 A Method for Transforming Temperature Distribution to Normality. Morris S. Webb, Jr., June 1977. (PB-271-742/AS)
123 Study of a Heavy Precipitation Occurrence in Redding, California. Christopher E. Fontana, June 1977. (PB-273-624/AS)
124 Statistical Guidance for Prediction of Eastern North Pacific Tropical Cyclone Motion - Part I. Charles J. Neumann and Preston W. Leftwich, August 1977. (PB-272-681)
125 Statistical Guidance on the Prediction of Eastern North Pacific Tropical Cyclone Motion - Part II. Preston W. Leftwich and Charles J. Neumann, August 1977. (PB-273-153/AS)
126 Climate of San Francisco. E. Jan Null, March 1978. (PB-278-975/AS)
127 Development of a Probability Equation for Winter-Type Precipitation Patterns in Great Falls, Montana. Kenneth B. Mielke, February 1978. (PB-281-387/AS)
128 Hand Calculator Program to Compute Parcel Thermal Dynamics. Dan Gudgel, April 1978. (PB-283-080/AS)
129 Fire Whirls. David W. Goens, May 1978. (PB-283-886/AS)
130 Flash-Flood Procedure. Ralph G. Hatch and Gerald Williams, May 1978. (PB-286-014/AS)
131 Automated Fire-Weather Forecasts. Mark A. Mollner and David E. Olsen, September 1978. (PB-289-916/AS)
132 Estimates of the Effects of Terrain Blocking on the Los Angeles WSR-74C Weather Radar. R. G. Pappas, R. Y. Lee, and B. W. Finke, October 1978. (PB-289-767/AS)
133 Spectral Techniques in Ocean Wave Forecasting. John A. Jannuzzi, October 1978.
134 Solar Radiation. John A. Jannuzzi, November 1978.
135 Application of a Spectrum Analyzer in Forecasting Ocean Swell in Southern California Coastal Waters. Lawrence P. Kieruff, January 1979.
136 Basic Hydrologic Principles. Thomas L. Dietrich, January 1979.
137 LFM 24-Hour Prediction of Eastern Pacific Cyclones Refined by Satellite Images. John R. Zimmerman and Charles F. Ruscha, Jr., January 1979.

NOAA SCIENTIFIC AND TECHNICAL PUBLICATIONS

NOAA, the *National Oceanic and Atmospheric Administration*, was established as part of the Department of Commerce on October 3, 1970. The mission responsibilities of NOAA are to monitor and predict the state of the solid Earth, the oceans and their living resources, the atmosphere, and the space environment of the Earth, and to assess the socioeconomic impact of natural and technological changes in the environment.

The six Major Line Components of NOAA regularly produce various types of scientific and technical information in the following kinds of publications:

PROFESSIONAL PAPERS — Important definitive research results, major techniques, and special investigations.

TECHNICAL REPORTS—Journal quality with extensive details, mathematical developments, or data listings.

TECHNICAL MEMORANDUMS — Reports of preliminary, partial, or negative research or technology results, interim instructions, and the like.

CONTRACT AND GRANT REPORTS—Reports prepared by contractors or grantees under NOAA sponsorship.

TECHNICAL SERVICE PUBLICATIONS—These are publications containing data, observations, instructions, etc. A partial listing: Data serials; Prediction and outlook periodicals; Technical manuals, training papers, planning reports, and information serials; and Miscellaneous technical publications.

ATLAS—Analysed data generally presented in the form of maps showing distribution of rainfall, chemical and physical conditions of oceans and atmosphere, distribution of fishes and marine mammals, ionospheric conditions, etc.

Information on availability of NOAA publications can be obtained from:

ENVIRONMENTAL SCIENCE INFORMATION CENTER
ENVIRONMENTAL DATA SERVICE
NATIONAL OCEANIC AND ATMOSPHERIC ADMINISTRATION
U.S. DEPARTMENT OF COMMERCE

3300 Whitehaven Street, N.W.
Washington, D.C. 20235